Proc. Natl. Acad. Sci. USA
Vol. 75, No. 11, pp. 5483–5487, November 1978
Biophysics

Conformational features of distamycin–DNA and netropsin–DNA complexes by Raman spectroscopy

(site-specific drugs/normal mode analysis/Raman difference spectra)

JAMES C. MARTIN, ROGER M. WARTELL, AND DONALD C. O'SHEA

School of Physics, Georgia Institute of Technology, Atlanta, Georgia 30332

Communicated by Elliott W. Montroll, August 4, 1978

ABSTRACT **The binding of distamycin and netropsin to duplex DNA has been studied by Raman spectroscopy. Several changes occur in the Raman spectra of these drugs upon binding DNA. These changes were analyzed by assigning specific motions to the observed Raman bands through the use of molecular subunits of the drugs and normal mode calculations. Our analysis indicates that pyrrole ring and peptide group vibrations are altered upon binding to DNA. The environments of the pyrrole ring methyl groups are not affected by the binding. These data provide physical evidence consistent with a binding model in which the methyl groups on the pyrroles project away from the DNA and the peptide N-H groups form hydrogen bonds with the DNA.**

Netropsin and distamycin A (Fig. 1) are related oligopeptide antibiotics that bind tightly to A·T-rich regions of duplex DNA. Many investigations (1–6) have yielded information about the mode of binding of these drugs to DNA. Solution studies show that these drugs do not unwind DNA upon binding (2, 7). The viscosity behavior of drug–DNA complexes indicates that netropsin elongates and stiffens DNA, whereas distamycin may bend the DNA helix (1, 8). Several results indicate that both drugs bind in the minor groove of DNA. (*i*) Both drugs bind tightly to the DNA polymers poly(dI)·poly(dC) and poly[(dI-C)]·poly[d(I-C)] in 0.1 M sodium ion solutions, but show little or no binding to poly(dG)·poly(dC) and poly[d(G-C)]·poly[d(G-C)] (2–4). These pairs of DNAs differ only at the 2 position of the purine ring, which lies in the minor groove. (*ii*) Adenine nitrogens in the minor groove of DNA are shielded from methylation by the binding of both drugs, while guanine nitrogens in the major groove remain unshielded (9). Estimates of the number of base pairs covered per drug molecule range from three to five (2, 5, 10) for netropsin.

These drugs are of interest because of their ability to recognize and bind to a specific feature of DNA. In this case the recognition feature consists of a region of high A·T composition. Thus, these drugs may serve as simple models for specific interactions between polypeptides and DNA. In addition, distamycin and netropsin show high antiviral activity (3). Clinical usefulness of these drugs has been limited by their toxicity. Information about their mode of binding can suggest chemical modifications which may decrease toxicity.

In this work we have studied the binding of distamycin and netropsin to DNA by Raman spectroscopy. We have obtained the Raman vibrational spectra of the drugs in the free state and when bound to DNA. By assigning bands of the drugs' Raman spectra to specific vibrations of these molecules, we were able to probe which portions of netropsin and distamycin are affected upon binding.

Our results show that pyrrole ring and peptide group vibrations are altered upon drug binding to DNA. The environment of the pyrrole ring methyl groups are not, however, affected by DNA binding. These data provide physical evidence for a binding model in which the methyl groups on the pyrroles project away from the DNA, and peptide N-H groups form hydrogen bonds with DNA.

The publication costs of this article were defrayed in part by page charge payment. This article must therefore be hereby marked "*advertisement*" in accordance with 18 U. S. C. §1734 solely to indicate this fact.

METHODS AND MATERIALS

Raman Instrumentation. A general description of the Raman spectrometer used has been presented (11). Major components of the system were a Coherent Radiation CR-6 argon ion laser, a Spex 1401 monochromator, and a cooled RCA 31034 selected photomultiplier. Signal pulses from the photomultiplier were amplified and then counted digitally by a scalar controlled by a PDP-8 f computer. The computer automatically coordinated the scanning of the spectrometer (effective slit width 4.5 cm^{-1}). Laser powers between 50 and 200 (mW) were used to examine drug and drug–DNA complexes. The 488-nm line of the argon laser was used. A quartz capillary equipped with a flat bottom was used as the sample cell; sample volumes were between 2.5 and 10 μl. The sample cell was held in an aluminum block whose temperature could be controlled by circulating water between 1° and 70°C. The laser beam entered the capillary through the bottom and scattered light was collected at 90° from the incident beam.

Materials. Netropsin samples were generously provided by N. Belcher (Pfizer), L. Ninet (Rhone Poulenc, France), F. Aracamone (Farmitalia, Italy), and E. L. Patterson (Lederle Laboratories). Distamycin A was obtained from Boehringer Mannheim. (See Fig. 1.) Netropsin samples, available in both sulfate and hydrochloride forms, were purified by repeated recrystallization into the sulfate form. Various concentrations of the drug were used up to its solubility limit. At room temperature this was about 0.7 mg/ml. The distamycin A samples required no purification to obtain high-quality spectra. Because the solubility of distamycin A is much greater than that of netropsin, concentrations up to 2.5 mg/ml could be used. Spectra were obtained from 100 to 2000 cm^{-1}. Care was taken to minimize the length of time the samples were irradiated by the laser. Raman spectra obtained at 25° and 1°C were not significantly different. Laser irradiation had no effect on the ultraviolet absorbance spectra of the samples. The drugs were dissolved in a 3–4 mM NaCl solution at pH 6.0–7.0. Calf thymus DNA, obtained from Sigma, was extracted with chloroform and sonicated, then extensively dialyzed with 1.0 mM NaCl. It was rotoevaporated to dryness and redissolved with double-distilled water to a final concentration of 6.0 mg/ml. The sodium ion concentration was approximately 3 mM. The polymer poly-[d(A-T)]·poly[d(A-T)] (gift of R. D. Wells, University of Wisconsin) was treated in a manner similar to the calf thymus DNA and used at a concentration of 4 mg/ml. Drug–DNA complexes were formed by mixing concentrated solutions of drug and DNA in a molar ratio of approximately 20 base pairs of DNA per drug molecule. The Raman spectra of each binding

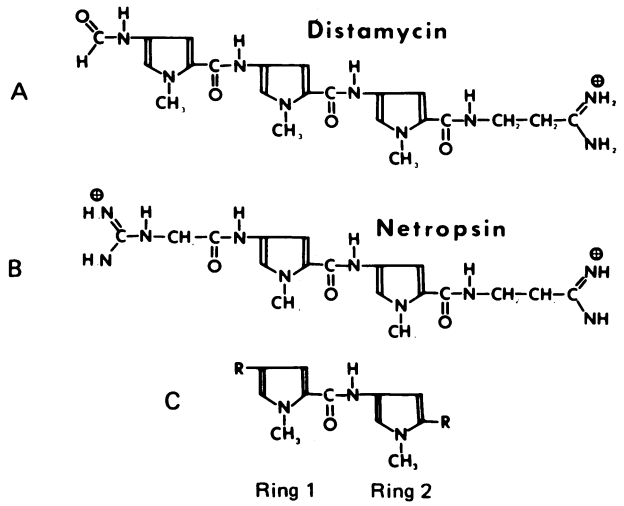

FIG. 1. Molecular structures of (*A*) distamycin, (*B*) netropsin, and (*C*) the molecular fragment examined in the normal mode calculations.

mixture were reproduced in three separate experiments. Pyrrole, *N*-methylpyrrole, and *N*-methylpyrrole-2-carboxaldehyde were obtained from Aldrich. In order to eliminate strong fluorescence interference, each was vacuum-distilled immediately before its spectroscopic use. The samples were protected from oxidation by a dry nitrogen atmosphere while their spectra were obtained.

Analysis Methods. Analysis of binding experiments required a careful comparison of the drug Raman bands in the presence and absence of DNA bands. This comparison was accomplished by subtracting variable amounts of one spectrum from another with the system's computer. The subtraction technique was used to normalize the various spectra to the same relative Raman intensity, with the 1645 cm^{-1} water band as an internal standard. The intensity of the water scattering measures the combined effect of experimental factors such as laser power, optical alignment, slit width, and counting time. Various amounts of a standard buffer spectrum were subtracted from an experimental spectrum until the water band was removed. The amount of the standard spectrum required to remove the water band provided a normalization for all experimental factors except sample concentration. Fig. 3 compares the spectrum of free distamycin with that of distamycin bound to calf thymus DNA. Both spectra have been normalized to the same Raman scattering intensity and drug concentration. The spectrum of unbound distamycin was obtained by subtracting the standard buffer spectrum from the distamycin–buffer spectrum. The spectrum of bound distamycin was obtained by a two-step process. Fractions of the standard buffer spectrum were separately subtracted from the spectrum of the distamycin–DNA mixture and of unbound DNA. A proportion of the resultant spectrum of the unbound DNA was then subtracted from the resultant distamycin–DNA spectrum until the DNA bands were removed. The latter procedure assumed that spectral differences between unbound and partially bound DNA were negligible. This is strictly correct for DNA bands unaffected by drug binding. It should also be approximately correct for other DNA bands given the 20:1 molar ratio of nucleotide pairs to drug. Additionally, only those DNA bands which overlap drug bands have the potential for significantly distorting the resultant spectrum. Two tests can be made for the procedure. One is the ability to remove all major DNA bands without distorting the background of the resultant spectrum. A second test is the correlation between observed changes in the bound compared with those in the free drug spectrum and the positions of DNA bands. Fig. 3 shows that the background of the bound and free distamycin spectra are undistorted and closely follow each other. Changes between the bound and free drug spectra do not correlate with the positions of DNA bands.

RESULTS AND DISCUSSION

The solution spectra of both netropsin and distamycin A are shown in Fig. 2. There is a general correspondence between the intensities and frequencies of many bands. This implies that these Raman bands arise from similar portions of the drugs. Several differences in frequency and relative intensity are noted in the 1175- to 1300-cm^{-1} region. One weak band occurs near 985 cm^{-1} in the spectrum of netropsin, but is absent in the spectrum of distamycin. Additional very weak lines were observed in the low-frequency spectrum of distamycin (not shown).

In order to draw conclusions about binding changes by Raman spectroscopy it is necessary to assign the observed Raman bands to corresponding normal modes of vibration. This assignment problem is complex for large molecules such as these drugs. When completed, however, each Raman band serves as a probe of what is happening to specific parts of the drug. Several techniques of increasing complexity were used to make assignments. Certain chemical groups within a large molecule have vibrational modes that are isolated by frequency and symmetry from the motions of the rest of the molecule (12). Thus, these frequencies are approximately characteristic of the group alone and may be transferrable to different molecules.

Table 1. Observed and calculated frequency shifts between pyrrole molecules, and assignments for *N*-methylpyrrole-2-carboxaldehyde

Pyrrole			*N*-Methylpyrrole			*N*-Methylpyrrole-2-carboxaldehyde	
ν_{OBS}	$\Delta\nu_{OBS}$	$\Delta\nu_{CALC}$	ν_{OBS}	$\Delta\nu_{OBS}$	$\Delta\nu_{CALC}$	ν_{OBS}	Assignment
601*	9	10	610	0	−7	610	C=C torsion
			667	31	35	698	Methyl stretch
826*	−3	−1	823	3	2	826	Ring H out of plane bend
876	2	2	878	10	25	888	Ring in plane bend
			971	55	47	1026	C-C stretch + ring H in plane bend
			1063	−7	−5	1056	Methyl rock
1148	−56	−56	1092	0	12	1092	Ring H in plane bend
1387	−1	0	1386	−12	8	1370	Ring stretch
1424	−38	−31	1386	1	5	1387	N-C stretch
			1422	−6	0	1416	Methyl bend
1532	−17	−10	1512	40	30	1522	C=C stretch

Frequencies (ν) are in cm^{-1}. ν_{OBS} are experimental frequencies. All vibrational modes are Raman active. $\Delta\nu_{OBS}$ and $\Delta\nu_{CALC}$ are the observed and calculated frequency shifts, respectively, between molecules for bands assigned to common vibrational modes.

* From studies of Scott (14). All other bands were observed by us.

This approach was used to find approximate frequencies for bands from the methyl and amide groups of netropsin and distamycin.

Information on the normal modes of the pyrrole rings and surrounding structures of the drugs was sought by investigating pyrrole, *N*-methylpyrrole, and *N*-methylpyrrole-2-carboxaldehyde. Some empirical correlations of lines were possible between these spectra based on chemical similarities and differences of the molecules. However, a more fundamental understanding of the vibrational characteristics of the molecules was required to correctly interpret their spectra.

Normal coordinate analyses were performed to help interpret the Raman spectra of the pyrrole molecules and the drugs. These calculations used a modified version of a program by Gwinn (13). In this program algebraic development of the vibrational problem is avoided by using a first principles approach. Mass-weighted cartesian coordinates are used, and the transformation between this system and the internal coordinates (in which the force constants are naturally defined) is performed numerically. Separation of rotation and translation occurs by the appearance of zero frequencies after diagonalization, eliminating the problems of redundant coordinates. Sections were added to the program to characterize the calculated normal modes by showing atomic motions and the potential energy distribution among the bond stretches, bends, and torsions. A more detailed description of the calculation will be presented elsewhere.

The key to any normal coordinate calculation is a physically realistic set of force constants. Force constants for individual bonds are not usually transferrable between molecules. However, they do have validity when viewed as a set that determines the vibrational motion of a specific group of connected atoms. Sets of force constants (or a force field) are developed from an initial trial set by an iterative procedure. The force field is varied until the difference between the calculated and experimental frequencies is minimized. Partial valence force fields determined in this way were available for pyrrole, *N*-methylpyrrole, and the peptide group (14, 15). These force fields were used to test our program. All predicted frequencies were within 1 cm^{-1} of values previously obtained for pyrrole, *N*-methylpyrrole, and *N*-methylacetamide using the Schactschneider normal coordinate analysis program (14, 15). The predicted frequencies and normal modes of *N*-methylpyrrole-2-carboxaldehyde were calculated by interfacing force constant sets for *N*-methylpyrrole and the carboxaldehyde group (16). Table 1 shows the calculated and observed frequency shifts between the pyrrole molecules along with the resulting assignments for *N*-methylpyrrole-2-carboxaldehyde. By comparing the calculated frequencies and normal modes for the pyrrole derivatives with their experimental frequencies from Raman spectra, we were able to follow spectral changes between these related molecules. Having information about the direction and approximate magnitude of such frequency shifts is essential for successfully assigning Raman bands. The good correlation between calculated and observed shifts in Table 1 confirms the success of this approach.

Based on our success with the pyrrole molecules, we used the same approach on a fragment of the drugs (shown in Fig. 1). The fragment contains two *N*-methylpyrrole rings coupled through a peptide linkage. This structure occurs in the central portion of both drugs. The inertial effects of the side chains (and the additional pyrrole on distamycin) are considered through effective masses. Force fields for *N*-methylpyrrole and the

Table 2. Observed frequencies for distamycin and calculated frequencies and modes for model fragment

Distamycin ν_{OBS}, cm^{-1}	Model fragment ν_{CALC}, cm^{-1}*	Mode
1010	998 (2), 1010 (1)	Interplane ring stretch and bend
1066	1059 (1), 1060 (2)	Methyl rock and pyrrole N-C stretch
1113	1113 (2), 1119 (1)	Methyl rock
1145	1152 (2), 1179 (1)	Interplane C-H bend and stretch; Interplane C-H bend
1209	1192 (1), 1195 (2)	Interplane C-H bend
1230	1224 (2)	Interplane C-H bend and stretch
1278	1278	Amide III
1354	1356 (1)	Interplane ring
1368	1360 (2)	C-C, C=C stretches
1396–1400	1398 (2), 1403 (1)	N-C ring stretch
1412	1408 (1, 2), 1409 (1, 2)	Methyl symmetric bend
1440	1437 (2), 1438 (1)	Methyl antisymmetric bend
	1452 (1, 2)	Methyl antisymmetric bend
	1452 (1, 2)	Methyl antisymmetric bend
1485	1481 (1), 1493 (2)	Ring N-C stretch
	1512 (1)	Ring C=C stretch
	1556 (2)	Ring C=C torsion
	1572 (2)	Ring C=C stretch
1583	1594	Amide and ring C=C stretch
1620–1640	1622, 1631	Ring C=C stretch
	1680	Amide I

* 1 and 2 refer to the pyrrole rings on the carboxyl and amide sides of the peptide link, respectively.

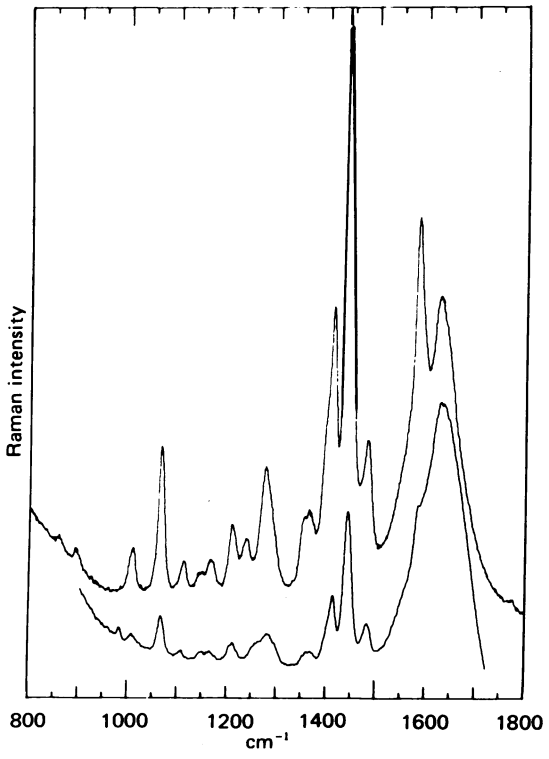

FIG. 2. Raman spectra of netropsin (*Lower*) and distamycin (*Upper*) in buffer. The two spectra shown are compared at the same relative intensity of the 1645 cm^{-1} water band.

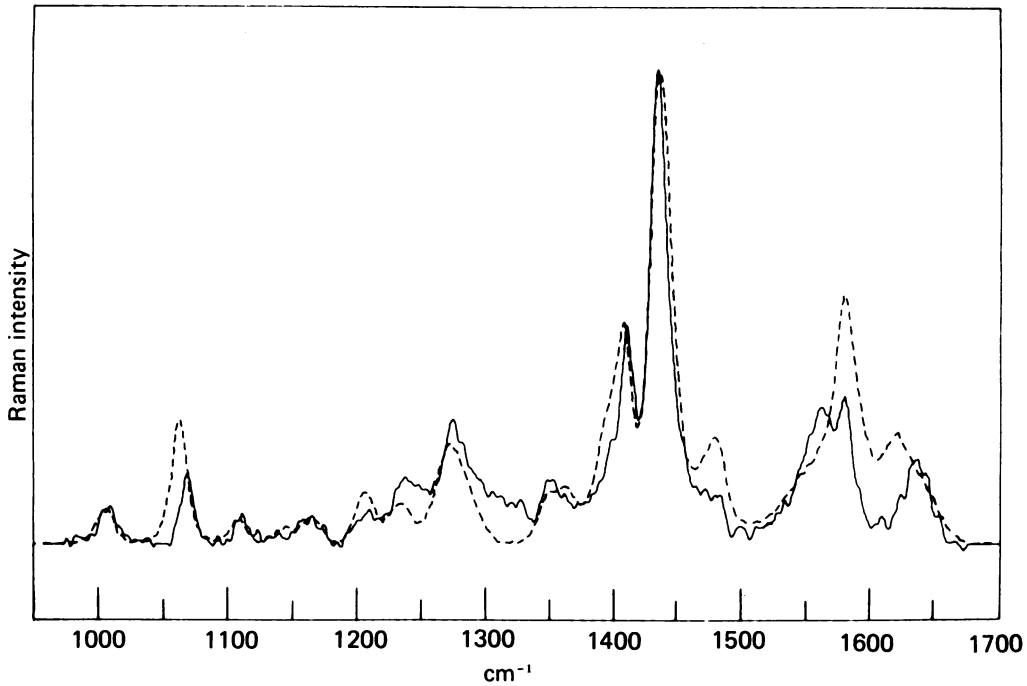

FIG. 3. Raman spectra of bound (—) and unbound (---) distamycin after subtraction of calf thymus DNA and buffer backgrounds and normalization to the same Raman scattering intensity and drug concentration.

peptide group were combined to describe this fragment. The combined partial valence force field contained terms connecting the pyrrole and peptide coordinates. Ring force constants were modified slightly to compensate for expected conjugation effects. The calculated frequencies for this fragment are shown in Table 2, together with a description of the normal modes. In this calculation both effective masses are set equal to 12 atomic mass units and the molecular backbone is specified to be planar (see Fig. 1). Varying the end masses from 12 to 80 atomic mass units and adjusting the dihedral angles of the fragment had a negligible effect on the frequencies of most normal modes. Frequency shifts were significant for a few lines whose assignments were already tentative and unimportant to the major conclusions of this work.

The frequencies of the distamycin A spectrum are also given in Table 2. The correspondence between observed and calculated frequencies is very good and leads to confident assignments for many observed lines. The strong band near 1440 cm^{-1} is assigned to a pure methyl antisymmetric bending mode. Calculated frequencies occur at 1437.0 and 1438.1 cm^{-1} for the vibrations of the two methyl groups. The adjacent band at 1412 cm^{-1} is assigned to a symmetric methyl band. The two calculated frequencies for this mode are at 1408.5 cm^{-1} and are split by only 0.5 cm^{-1}. Calculations show that for each of these two modes the potential energy is split in an approximate 30/70 ratio between the two methyl groups. Two additional lines are assigned to methyl rocking motions. These lines are observed at 1066 and 1113 cm^{-1} and calculated at 1060 and 1116 cm^{-1}, respectively. The calculated components of the latter frequency are split by 5 cm^{-1} and represent pure methyl rocking motion. The potential energy of the 1060 cm^{-1} mode is distributed between methyl rocking (60%) and various ring deformations (20% N-C stretches, 10% C-H in plane bends, etc.). The band observed at 1278 cm^{-1} is assigned to a mode that predominantly involves motions of the peptide group (amide III). The calculated mode was at the same frequency. Several bands are assigned to pyrrole ring deformations. Those occurring at 1010 cm^{-1} and around 1360 cm^{-1} involve mainly C-C stretching. At 1485 cm^{-1} a band is assigned mainly to ring N-C stretching with significant additional backbone deformations. Two additional modes involving mainly ring N-C stretching are calculated at 1398 and 1403 cm^{-1}. A shoulder of the 1412 cm^{-1} band is observed in this region. Subtraction of the broad water band near 1645 cm^{-1} (HOH bending) from the distamycin–buffer spectrum also indicates the presence of an additional band at 1630 cm^{-1} (see Fig. 3). Two pyrrole ring modes (predominately C=C stretch) are calculated to be at 1622 and 1631 cm^{-1}. These may give rise to the intensity noted in this region of the unbound distamycin spectra. The normal coordinate analysis predicts bands in the region between 1150 and 1225 cm^{-1} due to inplane bends of hydrogens attached to the pyrrole rings. Four weak bands observed in this region are therefore assigned as C-H inplane bends. For these four bands, however, the mean discrepancy between calculated and observed frequencies is 13 cm^{-1} compared to 4 cm^{-1} for the previous assignments, and hence must be considered more tentative. A strong band observed at 1583 cm^{-1} lies halfway between calculated frequencies at 1572 and 1594 cm^{-1}. Both calculated modes involve the stretching of ring bonds, while the latter also involves C-N and C=O stretching (32% potential energy distribution). Although a specific assignment of the 1583-cm^{-1} band cannot be made, it is likely to involve ring stretching.

Drug–DNA complexes

Fig. 3 shows the spectra of free distamycin and distamycin bound to calf thymus DNA. Comparison of the bound and unbound distamycin spectra shows that with the exception of the 1066 cm^{-1} band, all bands assigned to methyl vibrations remain unchanged. The intensity and position of the distamycin bands at 1412 and 1113 cm^{-1} and the strong 1440 cm^{-1} band are unaltered upon binding. The calculations of potential energy distribution indicate that these three modes involve purely methyl vibrations. The 1066-cm^{-1} band, which decreases by 60%, results from a mode that involves significant ring deformations in addition to methyl rocking. Thus the large change in this band is likely to be due to alterations in the vibrations of the pyrrole rings. This interpretation is supported by the ob-

servation that both bands assigned to ring N-C stretching (the shoulder at 1398 cm^{-1} and the band at 1485 cm^{-1}) show large intensity decreases in bound distamycin. In addition, the band at 1583 cm^{-1} splits into two components at 1567 and 1583 cm^{-1}. Unfortunately, the presence of a DNA band at 1581 cm^{-1} complicates the evaluation of the relative intensities of these two bands. Fig. 3 shows that if this DNA band remains unchanged upon drug binding, then the two bound drugs have equal intensities. Even if the DNA band did decrease, some change in the drug band is evident. In the unlikely case that the DNA band disappears completely upon drug binding, the 1583-cm^{-1} band would retain most of its intensity. However, the intensity at 1567 cm^{-1} would produce a distinct shoulder on the 1583-cm^{-1} band. Thus, some change at 1583 cm^{-1} must occur.

As shown in Fig. 3, there is a band near 1630 cm^{-1} in the unbound drug spectrum. This band shifts upward in frequency about 20 cm^{-1} upon binding. This shift appears to be real despite considerable noise due to the large water band subtracted from this region. Small changes occur in the bands at 1209, 1240, and 1278 cm^{-1}. The irregular nature and size of the changes and the overlapping of the DNA background makes it difficult to quantify these variations with confidence. The reproducible changes in intensity observed in the 1270- to 1340-cm^{-1} region may indicate an increase in the strength of the hydrogen bonds between the peptide N-H groups and hydrogen-bond acceptors (17). Chen and Lord (17) observed a correlation between an upward shift of the amide III band and increased hydrogen-bond strength for several homopolypeptides. The upward shift we observed is consistent with a change from N-H bonding with water to stronger hydrogen bonds with DNA. The changes of the bands at 1066, 1398, and 1485 cm^{-1} and the lack of change at 1412 and 1440 cm^{-1} were also observed in netropsin complexes with calf thymus DNA and $(dA\text{-}dT)_n\cdot(dA\text{-}dT)_n$. Because of the reduced drug solubility of netropsin compared to distamycin, the signal-to-noise ratios were smaller. Thus it was impossible to compare the variation in netropsin's weaker bands with their counterparts in distamycin.

Summary

The results provide physical evidence for several conformational features of netropsin–DNA and distamycin–DNA complexes. One characteristic is that the pyrrole ring methyl groups are unaffected by drug binding to DNA. Model-building studies indicate that this requires the methyl groups to project away from the DNA helix axis. Evidence in agreement with this finding is the observation that substitution of propyl groups at the 1 position of distamycin's pyrrole rings does not significantly alter its binding (18). Thus, pyrrole ring N-1 positions of these drugs are logical sites for chemical modifications aimed at creating cell uptake selectivity while maintaining DNA binding activity.

A second characteristic observed when the drugs bind to DNA is the change in pyrrole ring vibrational modes. Bands assigned to stretches of the ring N-C bands decrease substantially in intensity. These changes occur despite the absence of change in the nearby methyl groups. Since netropsin and distamycin do not unwind DNA and thus probably do not intercalate, it seems likely that direct interactions between other portions of the drugs and DNA induce a stress and/or alter bond orbitals in the pyrrole rings.

For distamycin, changes observed in the amide III region of the peptide groups are consistent with hydrogen bonding of peptide N-H groups to DNA. Although this conclusion is not unambiguous, involvement of the peptide N-H groups in binding to DNA is also suggested by model-building studies (unpublished observations; ref. 18). The netropsin Raman spectra was too weak in the amide III region to measure changes above the background variations. However, it seems likely from the other observations that hydrogen bonds between peptide N-H groups and DNA occur for netropsin also.

Support for this work is gratefully acknowledged from the Research Corporation (7188, to R.M.W.) and National Institutes of Health (GM24734, to R.M.W.).

1. Zimmer, Ch., Reinert, K. E., Luck, G., Wahnert, U., Lober, G. & Thrum, H. (1971) *J. Mol. Biol.* **58**, 329–348.
2. Wartell, R. M., Larson, J. E. & Wells, R. D. (1974) *J. Biol. Chem.* **249**, 6719–6731.
3. Zimmer, Ch. (1975) in *Progress in Nucleic Acid Research and Molecular Biology*, ed. Cohn, W. E. (Academic, New York), pp. 285–318.
4. Krey, A. K., Allison, R. G. & Hahn, F. E. (1973) *FEBS Lett.* **29**, 58–62.
5. Zasedatelev, A. S., Gursky, G. V., Zimmer, Ch. & Thrum, H. (1974) *Mol. Biol. Rep.* **1**, 337–342.
6. Patel, D. J. & Canuel, L. L. (1977) *Proc. Natl. Acad. Sci. USA* **74**, 5207–5211.
7. Luck, G., Triebel, H., Waring, M. J. & Zimmer, Ch. (1974) *Nucleic Acids Res.* **1**, 503–530.
8. Reinert, K. E. (1972) *J. Mol. Biol.* **72**, 593–607.
9. Kolchinskii, A. M., Mirzabekov, A. D., Zasedatelev, A. S., Gursky, G. V., Grokhovsky, S. L., Zhuze, A. L. & Gottich, B. P. (1975) *Mol. Biol. (Moscow)* **9**, 19–27.
10. Zimmer, Ch., Luck, G. & Fric, I. (1976) *Nucleic Acids Res.* **3**, 1521–1531.
11. Yu, N. T. (1977) *CRC Crit. Rev. Biochem.* **4**, 229–280.
12. Dollish, F. R., Fateley, W. G. & Bentley, F. F. (1974) *Characteristic Raman Frequencies of Organic Compounds* (Wiley and Sons, New York).
13. Gwinn, W. D. (1971) *J. Chem. Phys.* **55**, 477–481.
14. Scott, D. W. (1971) *J. Mol. Spect.* **37**, 77–91.
15. Jakes, J. & Krimm, S. (1971) *Spectrochim. Acta, Part A* **27**, 19–34.
16. Adamek, P., Volka, K., Ksandr, Z. & Stibor, I. (1973) *J. Mol. Spectrosc.* **47**, 252–267.
17. Chen, M. C. & Lord, R. C. (1974) *J. Am. Chem. Soc.* **96**, 4750–4752.
18. Zasedatelev, A. S., Zhuze, A. L., Tsimmer, K., Grokhovsky, S. L., Tumanyan, V. G., Gursky, G. V. & Gottich, B. P. (1976) *Dokl. Akad. Nauk SSR* **234**, 1006–1009.